

Volume 1, Issue 1 — January — June — 2017



E  
C  
O  
R  
F  
A  
N

**Journal-Taiwan**

ISSN-On line 2524-2121

**ECORFAN<sup>®</sup>**

**Indexing**

**Academic Google**



**ECORFAN<sup>®</sup> Taiwan**

## **ECORFAN-Taiwan**

### **Principal Directory**

RAMOS-ESCAMILLA, María. PhD.

### **Regional Director**

VARGAS-DELGADO, Oscar. PhD.

### **Director of the Journal**

PERALTA-CASTRO, Enrique. MsC.

### **Designer Edition**

CORTÉS-MUÑOZ, Sleither. BsC.

### **Editing Logistics**

FLORES-PIGUAVE, Sugely. BsC.

**ECORFAN Journal-Taiwan**, Volume 1, Issue 1, January-June -2017, is a journal edited semestral by ECORFAN ECORFAN-Taiwán. Taiwan, Taipei. YongHe district, ZhongXin, Street 69. Postcode: 23445. WEB: [www.ecorfan.org/taiwan/](http://www.ecorfan.org/taiwan/), [journal@ecorfan.org](mailto:journal@ecorfan.org). Editor in Chief: Ramos Escamilla- María. ISSN- 2524-2121. Responsible for the latest update of this number ECORFAN Computer Unit. Escamilla Bouchán-Imelda, Luna Soto-Vladimir, last updated June 30, 2017.

The opinions expressed by the authors do not necessarily reflect the views of the editor of the publication.

It is strictly forbidden to reproduce any part of the contents and images of the publication without permission of the National Institute of Copyright.

## **Editorial Board**

NAVARRO-FRÓMETA, Enrique. PhD.  
*Instituto Azerbaidzhan de Petróleo y Química*  
*Azizbekov, Russia*

BARDEY, David. PhD.  
*University of Besançon, France*

TORRES-CISNEROS, Miguel. PhD.  
*Universidad de Guanajuato, México*

RAJA-KAMARULZAMAN, Ibrahim. PhD.  
*Universiti Teknologi Malaysia, Malaysia*

BELTRÁN-PÉREZ, Georgina. PhD.  
*Benemérita Universidad Autónoma de Puebla,*  
*Mexico*

GARCÍA-RAMÍREZ, Mario Alberto. PhD  
*Universidad de Guadalajara, Mexico*

MAY-ARRIOJA, Daniel. PhD.  
*Centro de Investigaciones en Óptica, Mexico*

GUZMÁN-CHÁVEZ, Ana Dinora. PhD  
*Universidad de Guanajuato, Mexico*

VARGAS-RODRÍGUEZ, Everardo. PhD.  
*Universidad de Guanajuato, Mexico*

ESCALANTE-ZARATE, Luis. PhD.  
*Universitat de Valencia, Spain*

## **Arbitration Committee**

BMC. PhD.

*Universidad Industrial de Santander, Colombia*

BMLF. PhD.

*Universidad de Concepción, Chile*

RAG. PhD.

*University of Iowa, USA*

VMC. PhD.

*Universidad de Guanajuato, México*

RLR. PhD.

*Universidad de Guanajuato, México*

ASG. PhD

*Universidad Autónoma del Estado de Morelos*

MELO. PhD.

*Universidad Autónoma de San Luis Potosí, México*

GRMA. PhD

*Universidad de Guadalajara, México*

TANI. PhD.

*Centro de Investigaciones en Óptica, México*

JVD. PhD.

*Universidad de Guanajuato, México*

## Presentation

ECORFAN Journal-Republic of Taiwan is a research journal that publishes articles in the areas of:

### Applied Optics

In Pro-Research, Teaching and Training of human resources committed to Science. The content of the articles and reviews that appear in each issue are those of the authors and does not necessarily the opinion of the editor in chief.

In Number 1st presented the article Experimental investigation of a frequency swept laser based on erbium-doped fiber for applications in optical coherence tomography migrant by ARELLANO-ROMERO Silvia, BELTRAN-PEREZ, Georgina, CASTILLO, Mixcoatl, MUÑOZ-AGUIRRE, Severino, AVAZPOUR, Mahrokh, HERNANDEZ-GUTIERREZ, Ivan, RAMOS-BELTRAN, Jose de Jesus and MENDEZ-MARTINEZ, Hugo, with adscription in Benemerita Universidad Autónoma de Puebla, the next article name is Characterization of polarization-imbanced nonlinear loop mirror with input soliton pulses by AVAZPOUR, Mahrokh, BELTRÁN-PÉREZ, Georgina, RODRÍGUEZ-MORALES Luis, ESCAMILLA IBARRA, Baldemar and KUZIN, Evgeny with adscription in Benemerita Universidad Autónoma de Puebla, in the next Section the article Supercontinuum generation study through the RK4IP method by CARRILLO-DELGADO, Carlos Moisés, HERNANDEZ-GARCIA, Juan Carlos, ESTUDILLO-AYALA, Julian Moisés, LAUTERIO-CRUZ, Jesús Pablo, POTTIEZ, Olivier, MARTINEZ-ANGULO, José Ramón and ROJAS-LAGUNA, Roberto, adscripted on Universidad de Guanajuato, and the article A linear fiber laser temperature sensor based on a fiber Bragg grating by REYES-AYONA, Jose Roberto, TORRES-GONZÁLEZ, Daniel, JÁUREGUI-VÁZQUEZ, Natalia, ESTUDILLO-AYALA, Julián Moisés, SIERRA-HERNÁNDEZ, Juan Manuel, JÁUREQUI-VÁZQUEZ, Daniel, HERNÁNDEZ-GARCÍA, Juan Carlos and ROJAS-LAGUNA, Roberto, adscripted in Universidad de Guanajuato.

## Content

Article	Page
<b>Experimental investigation of a frequency swept laser based on erbium-doped fiber for applications in optical coherence tomography</b> ARELLANO-ROMERO Silvia, BELTRAN-PEREZ, Georgina, CASTILLO, Mixcoatl, MUÑOZ-AGUIRRE, Severino, AVAZPOUR, Mahrokh, HERNANDEZ-GUTIERREZ, Ivan, RAMOS-BELTRAN, Jose de Jesus and MENDEZ-MARTINEZ, Hugo	1-7
<b>Characterization of polarization-imbalanced nonlinear loop mirror with input soliton pulses</b> AVAZPOUR, Mahrokh, BELTRÁN-PÉREZ, Georgina, RODRÍGUEZ-MORALES Luis, ESCAMILLA IBARRA, Baldemar and KUZIN, Evgeny	8-13
<b>Supercontinuum generation study through the RK4IP method</b> CARRILLO-DELGADO, Carlos Moisés, HERNANDEZ-GARCIA, Juan Carlos, ESTUDILLO-AYALA, Julian Moisés, LAUTERIO-CRUZ, Jesús Pablo, POTTIEZ, Olivier, MARTINEZ-ANGULO, José Ramón and ROJAS-LAGUNA, Roberto	14-17
<b>A linear fiber laser temperature sensor based on a fiber Bragg grating</b> REYES-AYONA, Jose Roberto, TORRES-GONZÁLEZ, Daniel, JÁUREGUI-VÁZQUEZ, Natalia, ESTUDILLO-AYALA, Julián Moisés, SIERRA-HERNÁNDEZ, Juan Manuel, JÁUREQUI-VÁZQUEZ, Daniel, HERNÁNDEZ-GARCÍA, Juan Carlos and ROJAS-LAGUNA, Roberto	18-22

*Instructions for Authors*

*Originality Format*

*Authorization Form*

## Experimental investigation of a frequency swept laser based on erbium-doped fiber for applications in optical coherence tomography

ARELLANO-ROMERO Silvia†, BELTRAN-PEREZ, Georgina\*, CASTILLO, Mixcoatl, MUÑOZ-AGUIRRE, Severino, AVAZPOUR, Mahrokh, HERNANDEZ-GUTIERREZ, Ivan, RAMOS-BELTRAN, Jose de Jesus and MENDEZ-MARTINEZ, Hugo

*Benemérita Universidad Autónoma de Puebla, Cuerpo Académico de Optoelectrónica y Fotónica, Facultad de Ciencias Físico-Matemáticas.*

Received January 15, 2017; Accepted May 24, 2017

---

### Abstract

Nowadays, lasers based on erbium-doped fiber play an important role in different applications, such as optical coherence tomography (OCT) systems. An important part of these systems is the light source; in this case we focused on a frequency sweep source. One of the most important advantages of these systems is the possibility of obtaining images with only one sweep. This could be less tedious for the patient and less time consuming. In this work, we present the characterization and implementation of a frequency sweep source based on a ring cavity laser. The cavity used 30 cm of erbium ( $\text{Er } 16^+$ ) doped fiber as active medium with a total length of around 7 m. As a result, the maximum measured power was 9.5 mW in continuous wave. A Fabry-Perot filter was used to select the wavelength range, in this paper that range was between 1507 nm and 1584 nm to obtain a bandwidth of 77 nm. We characterized the suitable parameters needed to implement this cavity in an OCT system.

### Erbium-Doped, Optical Coherence, Frequency Swept, Laser Cavity

---

**Citation:** ARELLANO-ROMERO Silvia†, BELTRAN-PEREZ, Georgina\*, CASTILLO, Mixcoatl, MUÑOZ-AGUIRRE, Severino, AVAZPOUR, Mahrokh, HERNANDEZ-GUTIERREZ, Ivan, RAMOS-BELTRAN, Jose de Jesus, MENDEZ-MARTINEZ, Hugo. Experimental investigation of a frequency swept laser based on erbium-doped fiber for applications in optical coherence tomography. ECORFAN Journal-Taiwan. 2017, 1-1: 1-7

---

\* Correspondence to Author (email: gbeltran@cfm.buap.mx)

† Researcher contributing first author.



## Introduction

The optical coherence tomography (OCT) is recently one of the most demanded techniques in biomedical applications, since it is non-invasive for the patient. OCT is also a noncontact imaging modality that uses a coherent source to obtain high-resolution cross-sectional images of tissue microstructure (Fercher et. al. 2003). The 3-D microstructure image volume reveals more morphological information than 2-D images, which is critical in clinical applications such as early-stage cancer detection<sup>2</sup>. The OCT system uses a light source with low coherence and a Michelson interferometer (Drexler & Fujimoto, 2015). The light waves are sent through the biological tissue or other materials and the information is obtained from the interference between the light waves reflected by the tissue and the ones reflected by the mirror of the interferometer. For instance, with this technique, we could scan human tissue with high resolution of micrometers and a penetration depth of millimeters. There are two kinds of light sources that can be implanted in OCT systems, the time domain and Fourier domain. In the literature it is shown that OCT with frequency swept light source in the Fourier domain improve imaging speed over time swept sources. In this work we focused on a frequency swept source, a Fourier domain type. There are two main approaches used to build frequency swept, narrow linewidth light sources: The approach of “post-filtering” uses a broadband light source such as a superluminescent diode or a short pulse laser to generate a broad spectrum, then uses a narrowband tunable band-pass filter with a transmission window narrow enough for the desired instantaneous coherence length (Jianping et. al. 2008).. The approach of post filtering has the advantage that the tuning speed is limited only by the maximum tuning speed of the filter. However, the power of the light source is usually low, due to the high loss of the filtering process.

A complementary approach is “cavity-tuning”, where the spectral filtering element is used inside a laser cavity (Huang et.al. 1991). This last approach is the one used in this cavity, as in this way, we can feedback the cavity and improve the power obtained at the exit. Other frequencies swept sources have been built in different wavelengths range.

In this paper we present a ring cavity design of a frequency swept laser light source as well as its characterizations of power, spectrum and polarization, features that are important for proper use in OCT. We also present the characterization of the amplifier used at the end of the cavity with a gain of around 8 times of the input power. This cavity uses this amplifier to improve the output power going in the OCT for better imaging results. A Fabry-Perot filter is used as band-pass filter, working at 800 Hz. The amplifier also uses EDF as active medium. The purpose of the cavity presented is to be used in an OCT system for future purposes on early breast cancer detection.

## Experimental Setup

The experimental setup (Figure 1) consists of two parts, 1) erbium-doped fiber ring cavity and 2) the optical amplifier (Ramos-Beltrán, 2013). For the cavity we used a compact laser diode at 980 nm as a pump source (LD1, Compact LD driver by THORLABS, Inc.) which was coupled to the “A” port of a wavelength division multiplexer WDM1, (WDM by AFW, Inc.). The “C” port of the WDM1, which transmits at 1550 nm, was coupled to a 30 cm of erbium-doped fiber Er<sup>+</sup>16 (EDF1). In order to block the pump signal at 980 nm, the EDF1 was connected to the WDM2 (by AFW, Inc.). Afterwards, it is connected to an optical circulator (by AFW, Inc.) to prevent that the signal travels in the opposite direction.

ARELLANO-ROMERO Silvia†, BELTRAN-PEREZ, Georgina\*, CASTILLO, Mixcoatl, MUÑOZ-AGUIRRE, Severino, AVAZPOUR, Mahrokh, HERNANDEZ-GUTIERREZ, Ivan, RAMOS-BELTRAN, Jose de Jesus, MENDEZ-MARTINEZ, Hugo. Experimental investigation of a frequency swept laser based on erbium-doped fiber for applications in optical coherence tomography. ECORFAN Journal-Taiwan. 2017

The circulator is connected to a Fabry-Perot filter (FFP-TF2, Micron Optics, Inc.), which acts as a transmission filter to selecting the wavelength emission of the laser, the output of the Fabry-Perot goes to a coupler (optical coupler-90/10-0-N by AFW, Inc.) with a ratio of 90/10. The 10% of the signal is used as the feedback of the cavity while the 90% was used to measure the power and the spectrum of the output signal and also it is coupled to the amplifier (Figure 1).

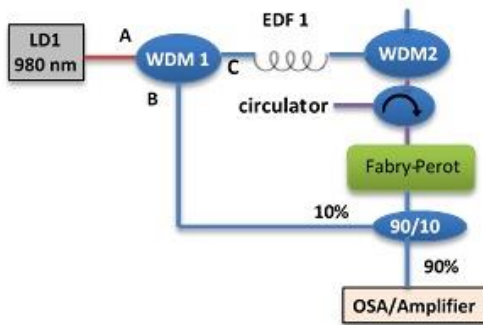


Figure 1. Experimental setup for ring cavity.

In figure 2 we show the experimental setup of the optical amplifier. The output of the cavity is connected to a circulator that goes to the “E” port of a WDM3 (by AFW, Inc.). The “D” port of the WDM3 receives the signal from a second compact laser diode (LD2) and the “F” port is connected to the EDF2 followed by the polarization controllers (PC, by THORLABS, Inc.) to maintain the polarization constant at the output of the system.

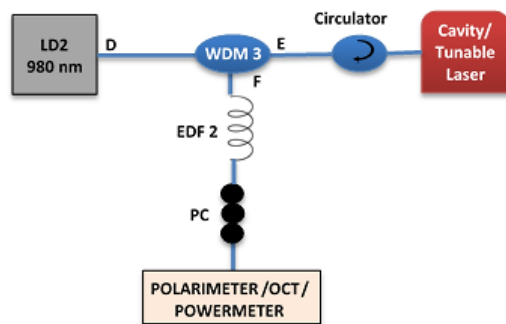
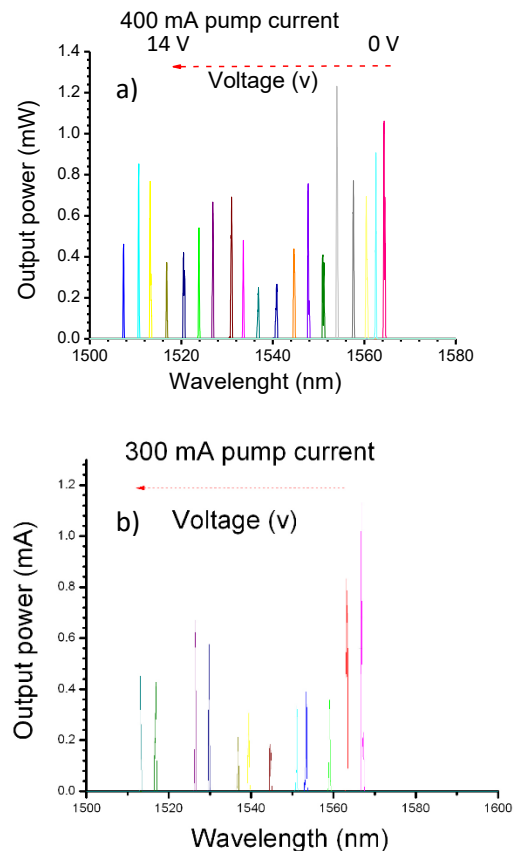


Figure 2. Experimental setup of the amplifier.

## Experimental methodology

Here the cavity was characterized in terms of the spectrum changes due to variations in either the pump current or the voltage of the Fabry-Perot. Results obtained are shown in Graphic 1. Moreover, in order to obtain these spectra, the output of the cavity was connected to an OSA (Optical spectrometry instrument by ScienceTech, Inc.) and the voltage was varied from 0 V to 14 V. Once the first peak of the spectrum appeared in the OSA we started to increment the voltage in 0.2 V intervals and its corresponding spectrum was recorded.

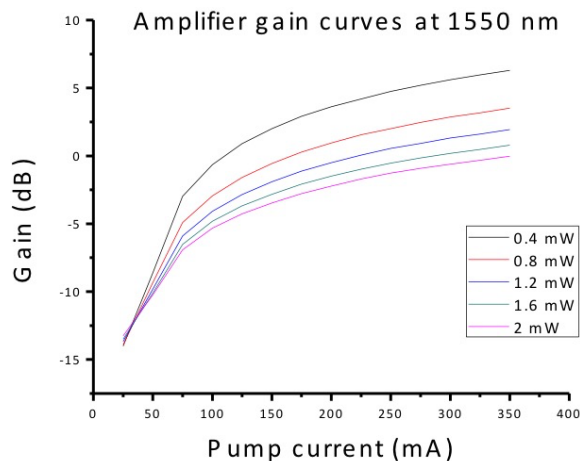


Graphic 1. Characterization of the spectrum at the end of the cavity for different voltage applied at the Fabry-Perot filter; a) LD1 at 400 mA; b) LD1 at 300 mA.

Now, in order to characterize the amplifier, we used a tunable laser. Firstly the output power of the amplifier was registered as we increased the tunable laser input power from 0.4 to 2 mW. Afterwards as we know the output ( $P_o$ ) and the input ( $P_i$ ) power the amplifier gain (Graphic 2) can be computed by using the following equation:

$$G = 10 \log \left( \frac{P_o}{P_i} \right) \quad (1)$$

The polarization of the signal of the amplifier was characterized by using a polarimeter for different pump currents from LD2 and different input powers of the tunable laser. The maximum gain was about 7 dB. Moreover, amplifier gain curves are shown in Graphic 2, where can be observed that the saturation power is beyond the maximum pump current of LD1 at 400 mA and that the signal is amplified almost 8 times.

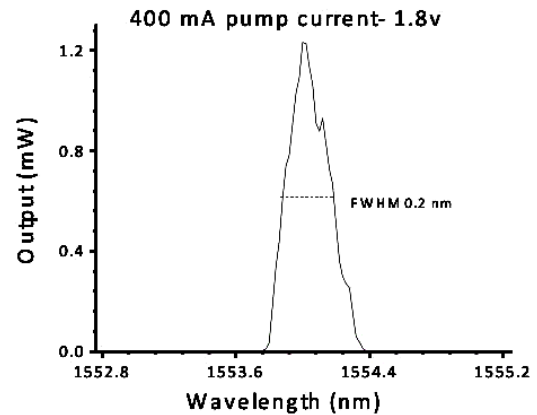


**Graphic 2.** Gain curves for the amplifier for different pump currents.

Once these steps were performed the the whole setup output as a function of the input power, the Fabry-Perot wavelength and the polarization were experimentally characterized.

## Results

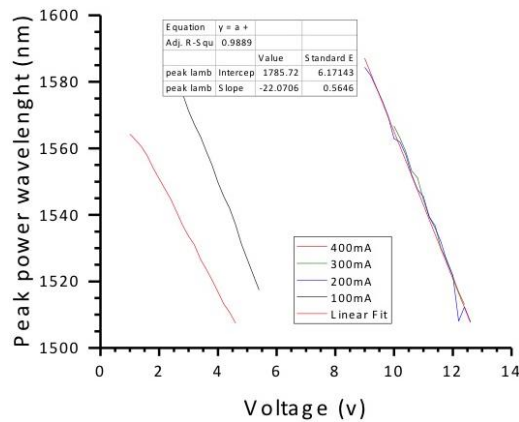
The laser emission after the cavity was measured with a power meter and it reached a peak of 1.2 mW at 400 mA input. After the amplifier, the maximum power obtained was 9.5 mW, nine times the signal of the cavity without the amplifier. The total spectrum obtained from the Fabry-Perot filter for all the different pumping powers moved between 1507 and 1584 nm, which represents a total bandwidth of 77 nm. In Graphic 3 it is shown a single peak spectrum with a full width at half maximum (FWHM) of 0.2 nm.



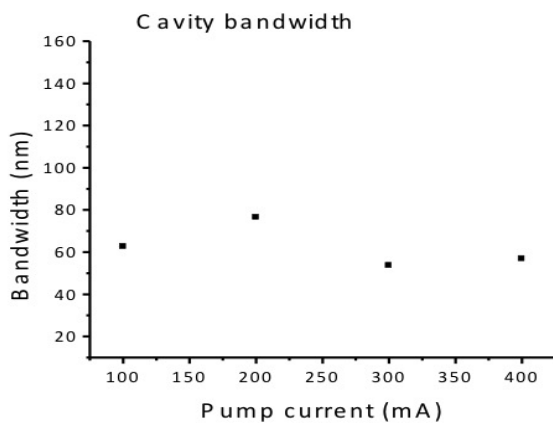
**Graphic 3** Single peak spectrum with a FWHM of 0.2 nm.

From the characterization procedure, it was observed that the wavelengths were shifted to the left as the voltage increased as described in Graphic 4. The wavelength shift versus the applied voltage has a linear relationships which do not change in a sensitive way if the current is varied. For instance we get an slope of -22 for 100 mA, 200 mA, and 300 mA and of -16.5 for 400 mA.

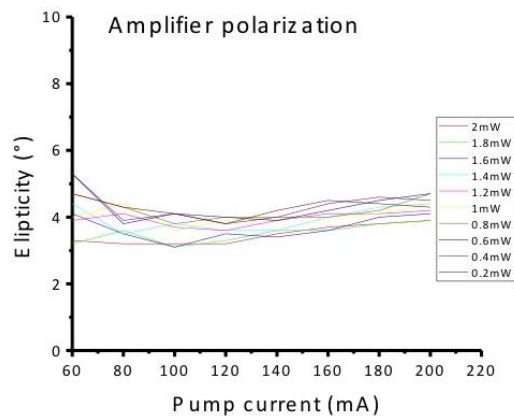
Another important issue that requires to be characterized is the bandwidth of each output spectrum. As can be seen in Graphic 5, the bandwidths were not much different among pump powers. The widest one was 77 nm for 200 mA and the narrowest one was 53 nm at 300 mA.



**Graphic 4.** Shows how the wavelegnth shift down when increasing the voltage of the Fabry-Perot filter.

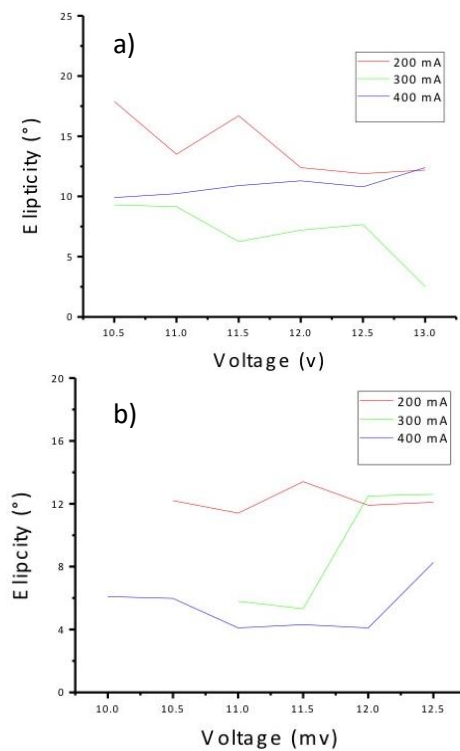


**Graphic 5.** Bandwidth of the whole spectrum for different pump currents.



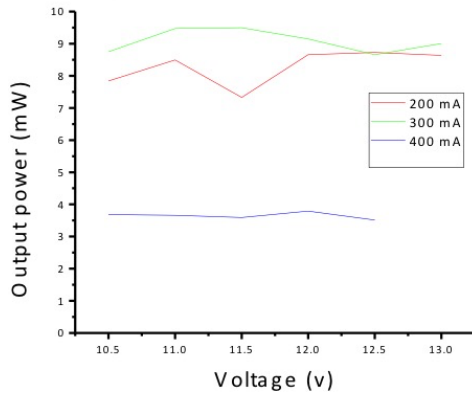
**Graphic 6.** Polarization at the output of the amplifier alone.

In the Graphic 6 the behavior of the polarization of the amplifier alone it is shown. Here can be noted that it remains constant for pump currents higher tan 80 mA and that it fluctuates for different input powers only by 1.5 degrees. Moreover, the polarization characterizaton of the overall experimental setup (cavity plus the amplifier) it is showed in Graphics 7, were can be appreciated that the ellipticity remains constant for the maximun current power of 400 mA, also remains constant when the voltage applied to the FPI within the range from 11.5 to 12.5 V at 300 mA.



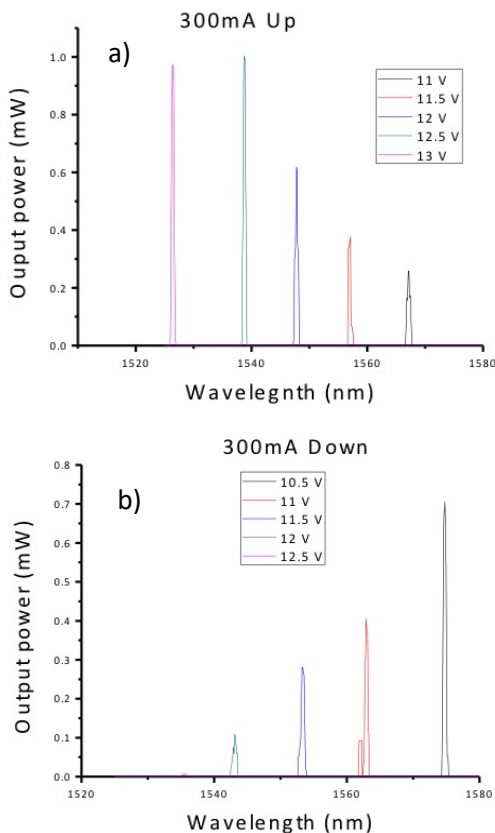
**Graphic 7.** Ellipticity changes as a function of the applied voltage to the Fabry-Perot filter in a) decreasing way and b) increasing way.

In Graphic 8, it is shown that the maximum power obtained is 9.5 mW and 3.7 mW for 300 and 400 mA respectively. These are the power levels in which we are interested since these are the current where the polarization remains constant.



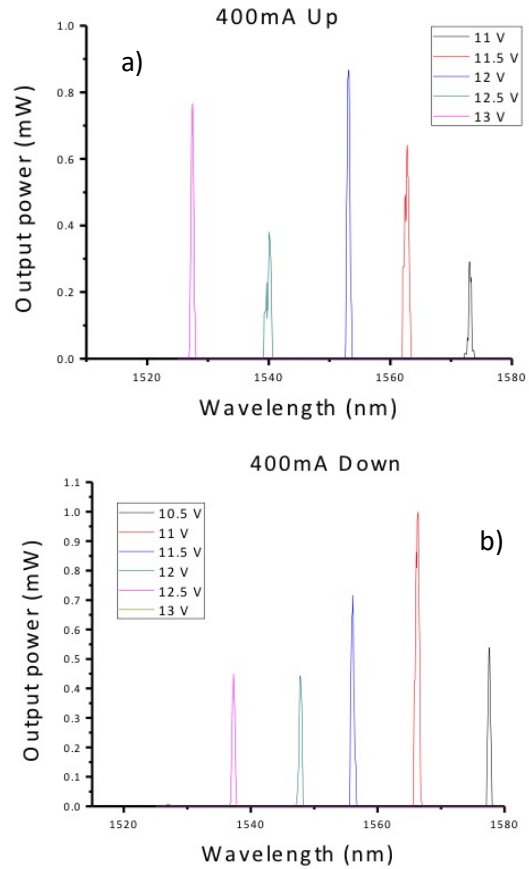
**Graphic 8.** Output power as the voltage applied to the Fabry-Perot filter is increased.

Moreover, spectra at the end of system formed by the cavity and the amplifier for 300 mA and 400 mA are shown in Graphic 9 and 10 respectively. Here the voltage was varied in both directions (increasing and decreasing the voltage).

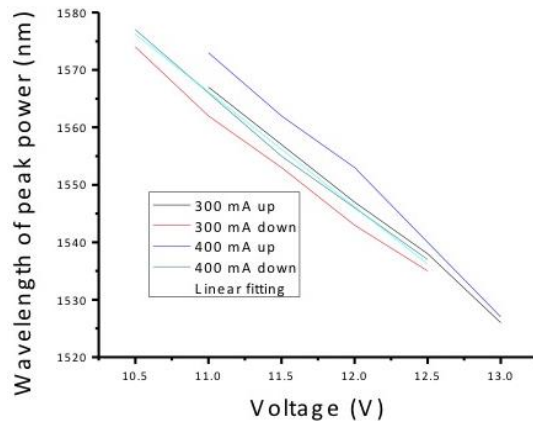


**Graphic 9.** Behaviour of the cavity and amplifier spectrum pumped with 300 mA and as the voltage is a) increasing and b) decreasing.

It is important to point out that the power levels showed in these graphics is approximately 40% of the total power since it is connected to the 40% part of the 40/60 coupler used. Additionally, from these graphics it can be seen that spectra for increasing the voltage and decreasing it are mirrors of each other, which tell us that the filter works in the same way for both directions. Hence, the output peak are shifted down in wavelength as the voltage is increased and it has the same behavior before reach the amplifier (Graphic 11).



**Graphic 10.** Behaviour of the cavity and amplifier spectrum pumped with 400 mA and as the voltage is a) increasing and b) decreasing.



**Graphic 11.** Wavelength shift down when the voltage of the Fabry-Perot filter increases, for the cavity and the amplifier.

## Conclusions

A frequency swept laser cavity based on erbium-doped fiber with a bandwidth of 77 nm at 200 mA was implemented. The maximum power obtained was 1.2 mW with a driver current of 400 mA. The bandwidth of each peak emission on continuous wave was about 0.2 nm. A characterization of the Fabry-Perot filter that is inside of the cavity was performed. An amplifier also based on erbium doped fiber was implemented, whose maximum output power was 9.5 mW. The ellipticity of the output signal fluctuates, in the best case, from around 3.5 to 5 degrees before the amplifier. After the amplifier ellipticity remains constant for pump current of 400 mA and a voltages from 10.5 v to 12.5 v which is adequate for the OCT system. Finally, we achieved a spectral swept power source that can be used in an OCT system for a possible application in the early detection of breast cancer.

## References

Drexler, W., & Fujimoto, J. G. (2015). *Optical coherence tomography: technology and applications*. Springer.

Fercher A. F., Drexler W., Hitzinger C. K. & Lasser T. (2003). Optical coherence tomography—principles and applications. *Reports in Progress in Physics* **66**(2), pp. 239

Huang D, Swanson EA, Lin CP, Schuman JS, Stinson WG, Chang W, Hee MR, Flotte T, Gregory K & Puliafito C.A. (1991). Optical coherence tomography. *Science* **254**, pp1178-81.

Ramos-Beltrán, J. J. (2013). Sistema de tomografía óptica coherente con un interferómetro de Michelson todo en fibra (Unpublished master's thesis). Facultad de ciencias Físico-Matemáticas, Posgrado en Física Aplicada, Benemérita Universidad Autónoma de Puebla.

Su J., Zhang J., Yu L., Colt H. G., Brenner M., & Chen Z. (2008). Real-time swept source optical coherence tomography imaging of the human airway using a microelectromechanical system endoscope and digital signal processor. *Journal of Biomedical Optics* **13**(3), pp. 030506

## Characterization of polarization-imbalanced nonlinear loop mirror with input soliton pulses

AVAZPOUR, Mahrokh<sup>†\*</sup>, BELTRÁN-PÉREZ, Georgina<sup>’</sup>, RODRÍGUEZ-MORALES Luis<sup>”</sup>, ESCAMILLA IBARRA, Baldemar<sup>”</sup> and KUZIN, Evgeny<sup>”</sup>

<sup>’</sup> Benemérita Universidad Autónoma de Puebla, Facultad de Ciencias Físico Matemáticas, Avenida San Claudio y 18 Sur, Colonia San Manuel, Ciudad Universitaria C.P. 72570 Puebla, México.

<sup>”</sup> Instituto Nacional de Astrofísica, Óptica y Electrónica, Enrique Erro 1, Tonantzintla, C.P. 72840 Puebla, México.

Received February 1, 2017; Accepted May 18, 2017

---

### Abstract

In this work we presented a simulation of the imbalanced-polarization non-linear loop mirror (NOLM) using a symmetrical coupler with a 50/50 ratio. Our aim of work is to find the soliton pulses in the output of the NOLM. A soliton is a pulse that maintains its shape while traveling at a constant speed. Solitons are caused by a compensation of nonlinear and dispersive effects in the medium. These kinds of pulses are important for many applications. The results showed that for the input powers of 650 W and 970 W for 200 m of fiber length in clockwise (CW) and counter clock-wise (CCW) directions respectively soliton pulses were obtained. We selected 800 W, as input power (peak power) for both directions (CW, CCW) to get soliton pulses at the output of the NOLM. With this power we obtained the spectra for different of fiber lengths; from 20 m to 1000 m. As a result for shorter length of fiber fewer fluctuations were obtained than the longer length. Furthermore for the shorter fiber length output spectrum were narrower than the longer fiber. Finally the transmission was less than 60% for longer fiber and around 90% for the shorter fiber.

### Nolm, Soliton, Imbalanced Polarization

---

**Citation:** AVAZPOUR, Mahrokh, BELTRÁN-PÉREZ, Georgina, RODRÍGUEZ-MORALES Luis, ESCAMILLA IBARRA, Baldemar, KUZIN, Evgeny. Characterization of polarization-imbalanced nonlinear loop mirror with input soliton pulses. ECORFAN Journal-Taiwan. 2017, 1-1: 8-13

---

\* Correspondence to Author (email: mahrokh.avazpour@gmail.com.)

† Researcher contributing first author.

## Introduction

The nonlinear optical loop mirror (NOLM) which is identified as Sagnac interferometer, firstly presented by Doran and Wood (Doran & Wood, 1988), that has been typically used in many important applications, such as optical processing and optical switching (Boscolo, Turitsyn, & Blow, 2008), wavelength demultiplexing (Sotobayashi, Sawaguchi, Koyamada, & Chujo, 2002), passive mode-locking (Duling, 1991), pedestal suppression and pulse compression (Pelusi, Matsui, & Suzuki, 1999), and regeneration of ultrafast data streams (Pelusi et al., 1999). In fact, the NOLM involves a coupler that output ports are linked by a fiber. For operation of NOLM it is necessary to reach the nonlinear phase shift between counter-propagating beams inside the fiber loop. There are several techniques to achieve this.

One is creating imbalanced power by using an asymmetrical coupler. Other is imbalanced dispersion using different special fibers inside in the loop. Furthermore there is imbalanced polarization by using symmetrical coupler and a quarter wave retarder (QWR) inside the loop of the NOLM (Armas-Rivera et al., 2016). This technique has many benefits compare to the other two techniques that we mentioned above. (Finlayson, Nayar, & Doran, 1992) and (Ibarra-Escamilla et al., 2006). The advantages of this are that low-power transmission depends on the angle of the QWR and it can be adjusted in the range between 0 and 0.5 by rotation the QWR. In order to operate the imbalanced polarization NOLM, we used at the input circular polarization pulses; in this case, clock wise direction (CW) of propagation in the loop has a circular polarization while the counter clock wise direction (CCW) has a linear polarization after passing the QWR.

Linearly polarized light accumulates a nonlinear phase shift which is 1.5 times larger than the circularly polarized light (Pottiez, Kuzin, Ibarra-Escamilla, & Mendez-Martinez, 2005). Furthermore, by using a rotation of QWR, the nonlinear transmission can be adjusted (Agrawal, 2001).

An optical soliton is a pulse that propagates inside the fiber without alteration, due to balance between nonlinear and dispersive effect (Blair, 1998). This is generated by a nonlinear phenomenon caused by self-phase modulation (SPM), which means that the electric field of the wave changes the index of refraction of fiber and the group velocity dispersion (Wiora, Weber, & Chanbai, 2013). The soliton pulse is important for different applications such as all-optical switching (Nishizawa & Goto, 2002). The minimum time-bandwidth product for a soliton is  $\approx 0.315$  for  $\text{sech}^2$ -shaped pulses and  $\approx 0.44$  for Gaussian-shaped pulses (Kivshar & Agrawal, 2003). This means that for a given spectral width, there is a lower limit for the pulse duration.

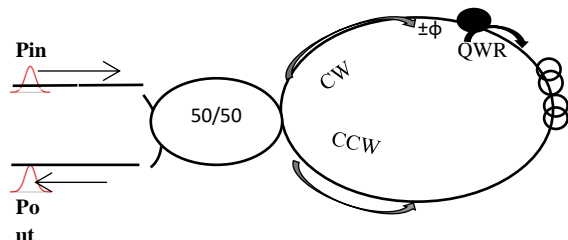
In the present work we simulate the imbalanced polarization NOLM by using a 50/50 coupler, and fiber squeezer as QWR. Moreover, a circular polarization soliton pulses considered as the input of the NOLM. In order to obtain soliton pulses at the output of the NOLM, we used 800 W as the input power peak. Moreover the study of different length of fibers shows different nonlinear transmission. In other words for longer length of fibers 200 m, the first maximum transmission was for 250 W as an input power with 60% of transmission with time band-width product of 0.28. For shorter of fiber length 20 m the maximum transmission was around 700 W as an input power with 90% of the transmission, with a time band-width product of 0.2.



## Experimental Setup

The experimental setup of imbalanced-polarization NOLM that we used in the

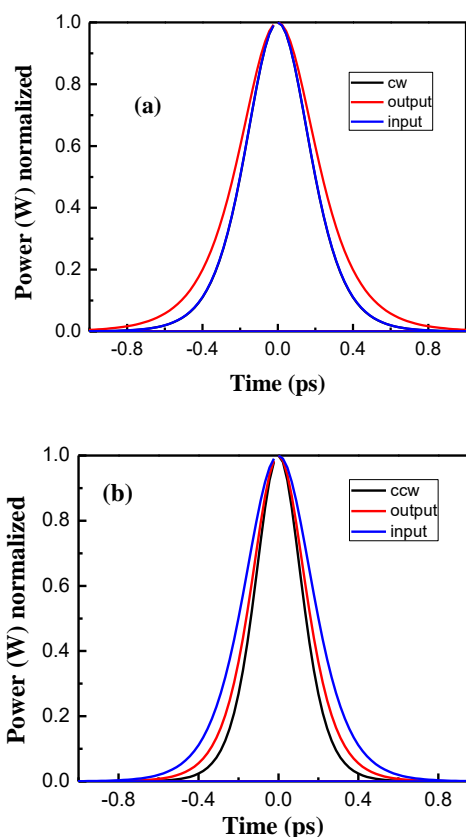
Simulation is shown in Fig. 1. It consists of a symmetrical coupler with a 50/50 coupling ratio and fiber squeezer as QWR. For the moment in our simulation QWR is composed of  $\theta=0$  for high transmission and high power and low transmission for low power, respectively. We used the second hyperbolic pulses with time duration of 0.4 ps and 1550 nm central wavelength as input signal. With this input pulse property we start to study and find the soliton pulses at the output. In order to obtain this we check the pulse performed as a soliton in CW and CCW directions respectively. At first, we consider the traveling of light inside the loop in CW direction passing through the QWR which converting the input polarization from circular to linear and it continues until it reaches to the output of NOLM. For the CCW direction the simulation procedure was similar to CW direction. The difference is CW direction the distance between the QWR and the input coupler is very short. It does mean that the intensity is 2/3 times less than the CW direction. With this difference we can produce the nonlinear phase shift. In our imbalanced polarization NOLM, different of fiber length inside de loop and different inputs power were considered. Moreover it is shown that the use of the symmetrical coupler allows very low transmission for low power.



**Figure 1:** Experimental Setup

## Results and discussion

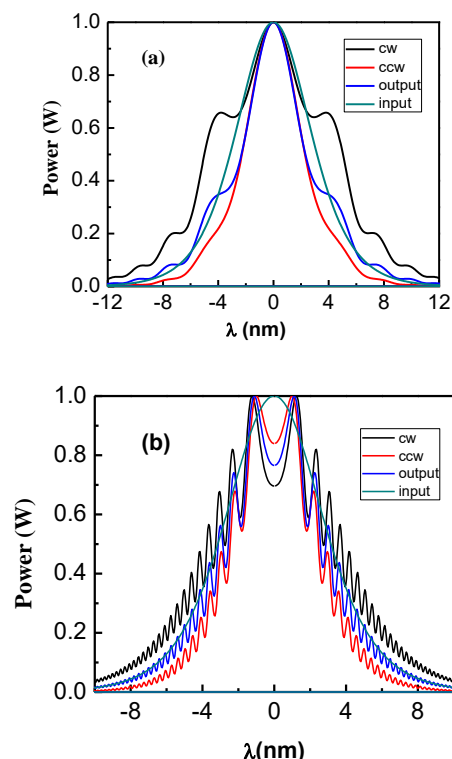
In figures 2a and 2b are shown the input soliton pulse (blue line), the output soliton pulse (red line) and the soliton pulse traveling in CW and CCW directions (black-line) for 200 m of fiber length and for input power of 650W and 970 W respectively. The results show that for CW direction the pulse duration is the same as input pulse soliton. However the output pulse shows a little broadening, it does mean that 650 W as an input power is not enough. Furthermore the results using 970 W as an input power shows that this power is more than power that need for soliton pulses because the pulse of output and CCW directions are compressed. Now we selected 800 W as an input power peak.



**Figure 2:** 200 m of fiber length a) CW direction, input power =650 W, b) CCW direction, input power=970

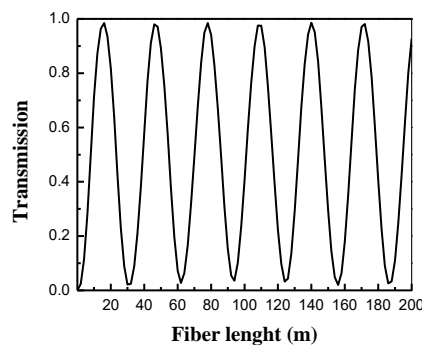
Moreover in Figure 3a and 3b are shown the spectra for two different lengths of fiber 20 m and 200 m with 800 W as input power. From Fig. 3a, it is clear that for CW direction (black line) there is broadening but in CCW (red line) and output (blue line) there are some compressing. The compressing in the spectrum is one point of our interest. Fig. 3b shows that the spectra of CW (black line) direction is wider than input spectra, however for CCW (red line) and output (blue line) there are compressing. Comparison of different length shows that there are less fluctuation for shorter fiber than longer fiber.

Figure 4 gives the result of transmission with for different fiber lengths from 0 m to 200 m, we calculate every 5 m of fiber length. In this case can find that only for 20 m of fiber is enough to reach the first maximum of transmission.

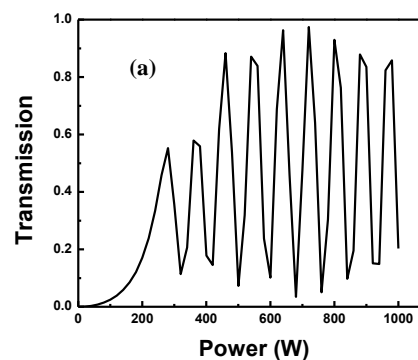


**Figure 3:** a) 20 m of fiber length, input Power 800 W, b) 200 m of fiber length, input power 800 W

Figures 5a and 5b show the transmission for 200 m and 20 m of fiber length with different power input from 0 W to 1000 W. From the figures it is clear that reaching to the first maximum transmission 60% for longer fiber length, we need less input power around 250 W. Though for the shorter fiber length reach to the maximum transmission 90%, we need almost three times more input power 700 W. In addition from this result, we calculate the time-bandwidth product, it was 0.2 and 0.28 for 20 m and 200 m respectively. As we already mentioned that the time-bandwidth is  $\approx 0.315$  for  $\text{sech}^2$ -shaped pulses, in our case time-bandwidth product is less than soliton pulses. We think that there is some compression in the output pulses of the NOLM.



**Figure 4:** Transmission for different of fiber length with input power 800 W



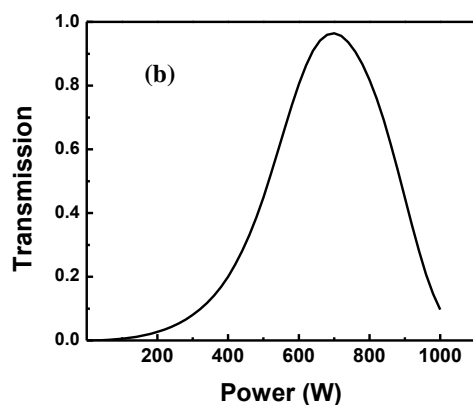


**Figure 5:** a) Transmission for different input power for 200 m of fiber length, b) Transmission for different input power for 20 m of fiber length.

## Conclusions

We have done our numerical simulation studies to get the soliton pulses at output of the imbalanced polarization NOLM. We studied different input power with different fiber length to find out suitable condition to get soliton pulses at the output of the NOLM. We measured the spectra for all input and output pulses. It is important to mention that in order to obtain soliton pulse at the output, the input power plays main role. We get that for 20 m, 700 W is required and the time-bandwidth was 0.2. Furthermore, for 200 m of fiber length the input power was 250 W and time-bandwidth product was 0.28.

## References

- Agrawal, G. (2001). *Applications of nonlinear fiber optics*. Academic press.
- Armas-Rivera, I., Rodriguez, Y. E. B., Perez, G. B., Aguirre, S. M., Pottiez, O., Escamilla, B. I., ... Carrascosa, A. (2016).
- Blair, S. M. (1998). Optical soliton-based logic gates.
- Boscolo, S., Turitsyn, S. K., & Blow, K. J. (2008). Nonlinear loop mirror-based all-optical signal processing in fiber-optic communications. *Optical Fiber Technology* **14**(4), 299–316.
- Doran, N. J., & Wood, D. (1988). Nonlinear-optical loop mirror. *Optics Letters* **13**(1), 56–58.
- Duling, I. N. (1991). All-fiber ring soliton laser mode locked with a nonlinear mirror. *Optics Letters* **16**(8), 539–541.
- Finlayson, N., Nayar, B. K., & Doran, N. J. (1992). Switch inversion and polarization sensitivity of the nonlinear-optical loop mirror. *Optics Letters* **17**(2), 112–114.
- Ibarra-Escamilla, B., Pottiez, O., Kuzin, E. A., Haus, J. W., Rojas-Laguna, R., Zaca-Moran, P., & Grajales-Coutino, R. (2006). Nonlinear Optical Loop Mirror with a Twisted Fiber and Birefringence Bias. In *Optical Communications, 2006. ECOC 2006. European Conference on* (pp. 1–2).
- Kivshar, Y. S., & Agrawal, G. (2003). *Optical solitons: from fibers to photonic crystals*. Academic press.
- Nishizawa, N., & Goto, T. (2002). Trapped pulse generation by femtosecond soliton pulse in birefringent optical fibers. *Optics Express* **10**(5), 256–261.

Pelusi, M. D., Matsui, Y., & Suzuki, A. (1999). Pedestal suppression from compressed femtosecond pulses using a nonlinear fiber loop mirror. *IEEE Journal of Quantum Electronics* **35**(6), 867–874.

Pottiez, O., Kuzin, E. A., Ibarra-Escamilla, B., & Mendez-Martinez, F. (2005). Theoretical investigation of the NOLM with highly twisted fibre and a  $\lambda/4$  birefringence bias. *Optics Communications* **254**(1), 152–167.

Sotobayashi, H., Sawaguchi, C., Koyamada, Y., & Chujo, W. (2002). Ultrafast walk-off-free nonlinear optical loop mirror by a simplified configuration for 320-Gbit/s time-division multiplexing signal demultiplexing. *Optics Letters* **27**(17), 1555–1557.

Wiora, G., Weber, M., & Chanbai, S. (2013). Optical Interferometry. In *Encyclopedia of Tribology* (pp. 2483–2488). Springer.

## Supercontinuum generation study through the RK4IP method

CARRILLO-DELGADO, Carlos Moisés†, HERNANDEZ-GARCIA, Juan Carlos\*, ESTUDILLO-AYALA, Julian Moisés, LAUTERIO-CRUZ, Jesús Pablo, POTTIEZ, Olivier, MARTINEZ-ANGULO, José Ramón and ROJAS-LAGUNA, Roberto

*Universidad de Guanajuato, División de Ingenierías Campus Irapuato-Salamanca, Carretera Salamanca-Valle de Santiago km 3.5+1.8 km, Comunidad de Palo Blanco, Salamanca, Gto., C.P. 36885, México.*

*\* Cátedras CONACyT, Av. Insurgentes Sur No. 1582, Col. Crédito Constructor, Del. Benito Juárez, C.P. 03940, México.*

*\*\*\* Centro de Investigaciones en Óptica (CIO), Loma del Bosque 115, Col. Lomas del Campestre, León Gto., 37150, México.*

Received January 11, 2017; Accepted May 8, 2017

### Abstract

In this paper we simulate the spectral broadening of an ultrashort pulse propagated into different lengths of standard single-mode fiber (SMF), by solving the generalized nonlinear Schrodinger equation (GNLSE), through the Fourth Order Runge–Kutta in the Interaction Picture (RK4IP) method. Here, it is possible to observe, by simulation or computational analysis, supercontinuum generation during the propagation of a pulse into a single mode optical fiber by the accumulation on nonlinear phenomena. Also, it is possible to predict its time and spectral behaviour.

### Supercontinuum Generation, Numerical Analysis, Nonlinear Optics

**Citation:** CARRILLO-DELGADO, Carlos Moisés; HERNANDEZ-GARCIA, Juan Carlos; ESTUDILLO-AYALA, Julian Moisés; LAUTERIO-CRUZ, Jesús Pablo; POTTIEZ, Olivier; MARTINEZ-ANGULO, José Ramón and ROJAS-LAGUNA, Roberto. Supercontinuum Generation in different lengths of SMF through the RK4IP method. ECORFAN Journal-Taiwan. 2017, 1-1: 14-17

\*Correspondance to Author (email: jchernandez@ugto.mx)

† Researcher contributing as first author.

## Introduction

Supercontinuum generation (SCG) is a nonlinear phenomenon as result of the sum of accumulative nonlinear effects. Although an optical fiber is made generally of silica and this material has a low nonlinear coefficient, the sum of all phenomena all along a large distance of fiber produces interesting phenomena, for instance solitonic effects, spectral broadening, and rogue waves (Akhmediev et al., 2013). The relevance to develop better supercontinuum light sources relies on their applications: optical communications, spectroscopy, optical pulse compression, imaging and microscopy, among others (Alfano, 2016). Our interest is focus to study the propagation of pulses through optical fibers with the purpose of generate flat spectrum and broadening spectrum (Estudillo-Ayala et al., 2012). In this paper, in a numerical way and through the RK4IP (Hult, 2007) algorithm, we achieved SCG using SMF with low peak powers (<5 W), as well as pulses of soliton shape (hyperbolic secant). Nonetheless, this study can be extended to non-common shapes like noise-like pulses (NLPs) and high energetic peak powers (>1 kW). Analyze and predict the behavior of pulses propagating in a SMF. Study how to produce or generate supercontinuum spectrum.

## Methodology

Pulse propagation through a medium implies the solution of the Nonlinear Schrödinger Equation (NLSE), or in our case, the Generalized (GNLSE). Rewriting the GNLSE in terms of the interaction picture method, we have, equation (1):

$$\frac{\partial A}{\partial z} = (\hat{D} + \hat{N})A \quad (1)$$

where  $A(z, T)$  is the complex field envelope in the  $z$  direction,  $T$  is the retarded time traveling at the envelope group velocity, and the operators  $\hat{D}$  and  $\hat{N}$  represent the dispersive and the nonlinear terms, respectively. The approximation is given at equation (2) and it is used for implementing the numerical method (Hult, 2007):

$$A_1 = \exp\left(\frac{h}{2}\hat{D}\right)A(z, T) \quad (2)$$

This method consists on separate the problem on different steps, where at the beginning the pulse start propagating into the medium, in our case an optical fiber of length  $L$ ; it is taken a piece of the fiber broken in a step  $h$  and the dispersion is solved at this point. So, this is, equation (3).

$$\begin{aligned} k_1 &= \exp\left(\frac{h}{2}\hat{D}\right)A(z, T)[h\hat{N}(A(z, T))]A(z, T) \\ k_2 &= h\hat{N}\left(A_1 + \frac{k_1}{2}\right)\left[A_1 + \frac{k_1}{2}\right] \\ k_3 &= h\hat{N}\left(A_1 + \frac{k_2}{2}\right)\left[A_1 + \frac{k_2}{2}\right] \\ k_4 &= h\hat{N}\left(\exp\left(\frac{h}{2}\hat{D}\right)(A_1 + k_3)\right) \\ &\quad \times \left(\exp\left(\frac{h}{2}\hat{D}\right)(A_1 + k_3)\right) \end{aligned} \quad (3)$$

The RK4IP method uses the Fast Fourier Transform (FFT) determining the dispersion effect in the frequency domain.

Then the field solution is transformed to give the final solution, which can be written as:

$$A(z + h, T) = \exp\left(\frac{\hbar}{2}\hat{D}\right)\left[A_1 + \frac{k_1}{6} + \frac{k_2}{3} + \frac{k_3}{3}\right] + \frac{k_4}{6} \quad (4)$$

As the parameters implemented for the computational study, we vary the length of the SMF: 1, 10 and 500 km; the fiber dispersion is  $D = 17$  ps/nm/km and the nonlinear coefficient is  $\gamma = 1.5/\text{W/km}$ .

## Results and Discussion

Figures 1 and 2 present simulations of the pulse propagating into the optical fiber; the results show, three stages of the same pulse only varying the length of the fiber, starting with 1 km, then 10 km and finally 500 km. The number of cycles for each computational case was 500.

In Fig. 1 is demonstrated the accumulation of nonlinear phenomena all along the length of the fiber (Agrawal, 2011), where by dispersive effects, is produced Self Phase Modulation (SPM). In the beginning of the SMF in Fig. 1(a), a solitonic effect is appreciated. Thus, energy travel slowly in the fiber generating the broadening of the spectrum, as depicted in Fig. 2. Something remarkable from the simulation are the dark regions where in between the center of the pulse originally propagating; those fringes remain at the lower energy by the total length of the fiber was 500 km (Fig 1(c)), is something than can be appreciated clearly in Fig 1(a) or 1(b).

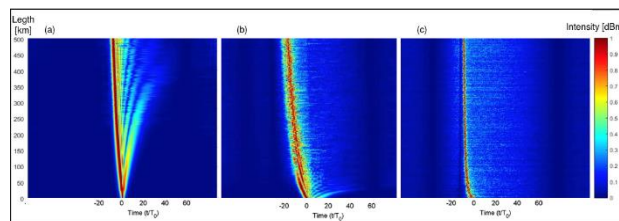


**Figure 1** Simulation of a hyperbolic secant pulse propagating into a single mode optical fiber with a peak power of 50 mW; (a) in the simulation of 1 km of fiber it can be appreciated solitonic effects; (b) in the simulation for 10 km, the energy of the pulse shifts to the blue, and appear new components; (c) for 500 km of fiber, the pulse shifts completely to a new temporal region, broadening the spectrum. At this point, it is important to note that are the dark or lower energies remain constant from all the fiber length.

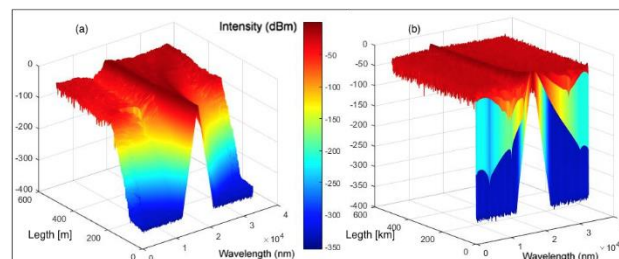


**Figure 2** Spectral behavior of the pulse, where is possible to appreciate the broadening of the spectrum, (a) in the 1 km case, (b) and in the 500 km case.

## Conclusions

In this work, through the RK4IP method, the spectral and temporal behavior of an ultrashort pulse, propagating into some pieces of SMF was shown. The simulated fiber lengths were 1, 10 and 500 km. Nonlinear phenomena were formed such as: solitonic effects, spectral broadening, and SPM. The wavelength was centered on 1550 nm, and the peak power was 50 mW. Those parameters were proposed, to get an approach on than we could have experimentally.

## Acknowledgments

C.M. Carrillo-Delgado was supported by the CONACyT grant No. 245146. This work was funded by Cátedras-CONACyT project 3155 and Ciencia Básica project No. 257691.

**References**

Agrawal, G. P. (2011). Nonlinear fiber optics: its history and recent progress. *Journal of the Optical Society of America B* 28(12), pp. A1-A10.

Akhmediev, N., Dudley, J. M., Solli, D. R. & Turitsyn, S. K. (2013). Recent progress in investigating optical rogue waves, *Journal of Optics* 15(6), 060201.

Alfano, R.R. “The Supercontinuum Laser Source: The Ultimate White Light”, 3th ed. (Springer, 2016).

Estudillo-Ayala, J., Rojas-Laguna, R., Hernandez-Garcia, J. C., Pottiez, O., Mata-Chavez, R., Trejo-Duran, M., Jauregui-Vazquez, D., Sierra-Hernandez, J. M. & Andrade-Lucio, J. (2012). Supercontinuum generation in standard telecom fiber using picoseconds pulses. *Proceedings of SPIE* 8240, 82401G

Hult, J. (2007). A fourth-order Runge–Kutta in the interaction picture method for simulating supercontinuum generation in optical fibers, *Journal of Lightwave Technology* 25(12), pp. 3770-3775.



## A linear fiber laser temperature sensor based on a fiber Bragg grating

REYES-AYONA, Jose Roberto†, TORRES-GONZÁLEZ, Daniel, JÁUREGUI-VÁZQUEZ, Natalia, ESTUDILLO-AYALA, Julián Moisés, SIERRA-HERNÁNDEZ, Juan Manuel, JÁUREQUI-VÁZQUEZ, Daniel, HERNÁNDEZ-GARCÍA, Juan Carlos and ROJAS-LAGUNA, Roberto\*.

*Universidad de Guanajuato, Departamento de Ingeniería Electrónica, División de Ingeniería Campus Irapuato-Salamanca, Carretera Salamanca-Valle de Santiago km 3.5+1.8, Comunidad de Palo Blanco, C.P. 36885. Salamanca, Gto.*

Received January 30, 2017; Accepted May 28, 2017

### Abstract

In this work, a linear fiber laser temperature sensor based on a fiber Bragg grating (FBG) is presented. Here, a microchip Q-switched laser working at 1064 nm is used. Additionally, a fiber Bragg grating is used as head sensing and its wavelength is centered at 1550 nm. Moreover, the linear laser can be tunable from 1548 to 1553 nm when the temperature is varied, and a sensitivity of 58.33 °C/nm is achieved in a range from 3 to 200 °C. The supercontinuum (SC) generation was achieved by means of the pulsed laser and bending of SMF-28 fiber in a cylindrical tube.

### Sensors, Fiber Bragg Grating, Supercontinuum Generation

**Citation:** REYES-AYONA, Jose Roberto†, TORRES-GONZÁLEZ, Daniel, JÁUREGUI-VÁZQUEZ, Natalia, ESTUDILLO-AYALA, Julián Moisés, SIERRA-HERNÁNDEZ, Juan Manuel, JÁUREQUI-VÁZQUEZ, Daniel, HERNÁNDEZ-GARCÍA, Juan Carlos and ROJAS-LAGUNA, Roberto\*. A linear fiber laser temperature sensor based on a fiber Bragg grating. ECORFAN Journal-Taiwan. 2017, 1-1: 18-22

\* Corresponding Author (email: rlaguna@ugto.mx)

† Researcher contributing as first author.

## Introduction

Optical fiber sensors have been studied in the past few decades due to their immunity to electromagnetic interference, high sensitivity and capability of measure in situations where conventional electronic or electro-mechanical sensors would be affected by, for example, a harsh environment (Grattan & Sun, 2000). One way to approach optical fiber temperature sensors is by means of interferometric sensors, such as the proposed by Martinez-Rios et al. whose experimental setup presents an Erbium-doped fiber ring laser with a Mach-Zehnder interferometer as sensing element placed in different solutions of glycerol and water, showing a maximum sensitivity of 1089 pm/°C in a temperature range from 55 to 70 °C (Martinez-Rios et al., 2015).

Other temperature sensors have been studied by using other kind of optical devices, such as Fabry-Perot interferometers (Pinto et al., 2010), multimode interference (Nguyen et al., 2008) and photonic crystal fiber (PCF) (Yang, Lu, Liu & Yao, 2017). Fiber grating sensors are commonly used because of their high sensitivity, which can be increased with the use of an interferometer. As an example, the experimental setup proposed by Gonzalez-Reyna et al. (2015) presented a sensitivity of 18.8 pm/°C within the range from 220 to 90 °C. Another advantage fiber grating sensors present is their multiplexing capability (Kersey et al., 1997; Mandal et al., 2006). Furthermore, supercontinuum is the nonlinear process of spectral broadening of light and has found applications in telecommunications, sensing and spectroscopy.

Supercontinuum generation can be produced through the interaction of linear effects such as dispersion, and nonlinear propagation effects such as self-phase modulation (SPM), cross-phase modulation (XPM), Raman scattering, four-wave mixing (FWM), modulation instability (MI) and others (Dudley & Taylor, 2010). Efficient SC can be achieved by using pulses in the order of femtoseconds and a peak power of kW through optical fiber.

A well-known feature that optical fibers have, is the nullification of dispersion in a specific wavelength. This wavelength is named zero-dispersion wavelength and is denoted as  $\lambda_0$ . Above this wavelength ( $D > 0, \beta_2 < 0$ ) the optical fiber presents an anomalous dispersion regime, while below this wavelength ( $D > 0, \beta_2 > 0$ ) propagation takes place in the normal dispersion regime. In past works, it has been demonstrated that depending on the characteristics of the pumping beam employed in the supercontinuum generation, is the contribution of the nonlinear effects involved (Gutierrez-Gutierrez et al., 2009; Estudillo-Ayala et al., 2012). In this work, we are using standard SMF-28 optical fiber with a zero-dispersion wavelength at 1310 nm and a pumping source operating at 1064 nm. Therefore, the experiment happens in the normal dispersion regime, thus, the linear and nonlinear effects involved in the supercontinuum generation are: group velocity dispersion (GVD), self-phase modulation (SPM), modulation instability (MI) and stimulated Raman scattering (SRS).

The objective of this study was to develop a simple, reliable and cost-efficient fiber laser configuration using only a FBG as the sensing and tuning element.

## Experimental setup

The proposed laser configuration is shown in Figure 1. A microchip Q-switched laser operating at 1064 nm with a peak power of 10 kW, pulses of 700 ps and 9kHz repetition frequency (Teem Photonics, microchip model:

MNP-06E-100) was coupled to the port 1 of a four-port 99/1 coupler by means of a mirror and a 10X microscope objective mounted on a manual XYZ stage. Port 3, with 99% of laser's power is connected to 100 m of SMF-28 fiber wrapped to a 5.4 cm diameter cylindrical tube. Additionally, the bending of SMF-28 fiber through the cylindrical tube acted as our nonlinear medium. This section was spliced to the FBG which represents one end of the configuration and whose Bragg wavelength is centered at 1550 nm. On port 2 of the coupler, a circulator is connected, completing the laser cavity. The output power was measured with an optical spectrum analyzer (OSA, Yokogawa AQ6370B) through a 90/10 coupler placed on the circulator loop. Additionally, OSA resolution used was 0.1 nm.

From below 24 °C, the FBG was placed on a Peltier cell and from above 24 °C, the FBG was placed on an electric oven. Temperature was monitored by means of a thermocouple and a multimeter (Tektronix TX-DMM TX3 digital multimeter) in both cases.

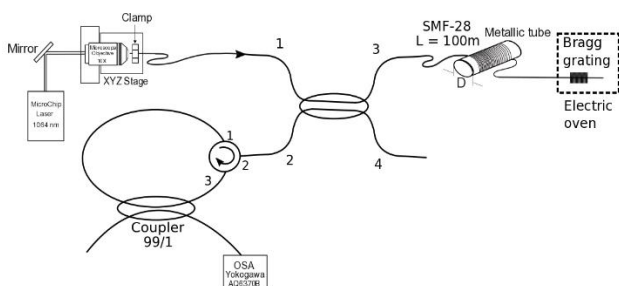


**Figure 1** Experimental setup of the temperature sensor.

It is important to point out that the diameter selection of the cylindrical tube was due to good stability response and sufficient spectral broadening for our experiment (Rojas-Laguna et al., 2015).

## Results and discussion

Broad spectral fiber laser due to supercontinuum generation observed between the 100 m of SMF-28 and the FBG is shown in Figure 2. The SC spectra goes from 1064 nm to 1660 nm. Fiber laser output spectral responses to temperature changes are shown in Figure 3. Wavelength shifts as well as a slight variation of the output power can be observed. Wavelength displacement can be explained by the temperature dependence of the refractive index of the FBG. In addition, Figure 4 shows the maximum output power wavelength, or peak wavelength, at different temperatures. Note how the Bragg wavelength is centered on 1550 nm at 24 °C, as mentioned before. Moreover, the wavelength shift of the sensor shows a quasi linear response to the temperature changes in a range from 3 to 200 °C with a sensitivity of 58.33 °C/nm. Comparing Figure 3 and Figure 4, temperature sensors show a wavelength displacement from left to right.

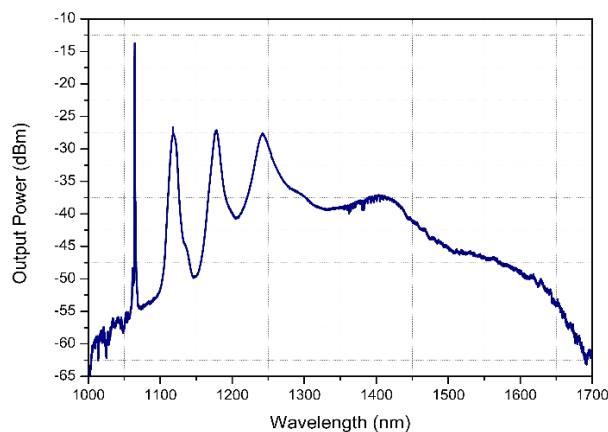


**Figure 2** Supercontinuum spectra generated.

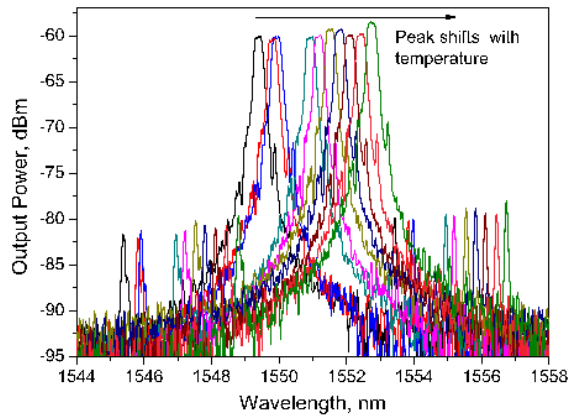


Figure 3 Output laser spectrum at different temperatures.

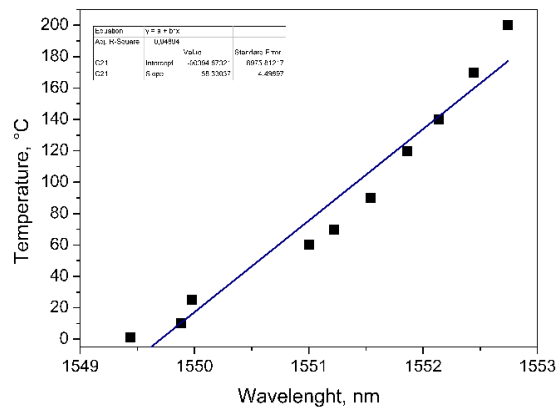


Figure 4 Output laser spectral peaks at different temperatures.

## Conclusions

In this paper, a linear fiber laser temperature sensor based on fiber Bragg grating with a SC source has been demonstrated. A linearly sensitivity of 58.33 °C/nm in the ranges from 3 to 200 °C demonstrates a high sensitivity and stability at room temperature considering the experimental setup proposed. SC generation was achieved by means of a pulsed microchip Q-switched laser and bending 100 m of the SMF-28 fiber on the cylindrical tube.

Finally, due to the lack of use of special optical fiber components such as rare-earth-doped fiber, photonic crystal fiber and interferometers, the temperature sensor has a low cost and a simple fabrication process.

## Acknowledgement

This work was supported by the National Council for the Science and Technology (CONACyT) under Project 183893. Daniel Torres-González would like to thank Universidad de Guanajuato for a student research scholarship.

## References

- Dudley, J. M. & Taylor, J. R. (2010). Supercontinuum generation in optical fibers. Cambridge, New York: Cambridge University Press.
- Estudillo-Ayala, J. M., Rojas-Laguna, R., Hernandez-Garcia, J. C., Pottiez, O., Mata-Chavez, R. I., Trejo-Duran, M., Jauregui-Vazquez, D., Sierra-Hernandez, J. M. & Andrade-Lucio, J. A. (2012). Supercontinuum generation in standard telecom fiber using picoseconds pulses.
- Gonzalez-Reyna, M. A., Alvarado-Mendez, E., Estudillo-Ayala, J. M., Vargas-Rodriguez, E., Sosa-Morales, M. E., Sierra-Hernandez, J. M., Jauregui-Vazquez, D. & Rojas-Laguna, R. (2015). Laser Temperature Sensor Based on a Fiber Bragg Grating. *IEEE Photonics Technology Letters* **27**(11), pp. 1141-1144.

Gutierrez-Gutierrez, J., Vargas-Treviño, M., Romero-Salazar, C., Hernandez-Flores, O. A., Kuzin, E. A., Ibarra-Escamilla, B., Grajales-Coutiño, R., Rojas-Laguna, R., Estudillo-Ayala, J. M., Vargas-Rodríguez, E., & Gutierrez-Zainos, F. (2009).

Influencia de la inestabilidad modulacional en la generación de un espectro continuo en fibras ópticas con pulsos de nanosegundos. *Revista Mexicana de Física* **55**(5), pp. 359-366.

Grattan, K. T. V. & Sun, T. (2000). Fiber optic sensor technology: an overview. *Sensors and Actuators A: Physical* **82**(1), pp. 40-61.

Kersey, A. D., Davis, M. A., Patrick, H. J., LeBlanc, M., Koo, K. P., Askins, C. G., Putnam, M. A., & Friebele, E. J. (1997). Fiber grating sensors. *Journal of Lightwave Technology* **15**(8), pp. 1442-1463.

Mandal, J., Sun, T., Grattan, K., Zheng, R., Ngo, N., & Augousti, A. (2006). A Parallel Multiplexed Temperature Sensor System Using Bragg-Grating-Based Fiber Lasers. *IEEE Sensors Journal* **6**(4), 986-995.

Martinez-Rios, A., Anzueto-Sanchez, G., Selvas-Aguilar, R., Guzman, A. A. C., Toral-Acosta, D., Guzman-Ramos, V., Duran-Ramirez, V. M., Guerrero-Viramontes, J. A. & Calles-Arriaga, C. A. (2015). High Sensitivity Fiber Laser Temperature Sensor. *IEEE Sensors Journal* **15**(4), pp. 2399-2402.

Nguyen, L. V., Hwang, D., Moon, S., Seung Moon, D., & Chung, Y. (2008). High Temperature Fiber Sensor with Sensitivity Based on Core Diameter Mismatch. *Optics Express* **16**(15), pp. 11369-11375.

Pinto, A. M. R., Frazo, O., Santos, J. L., Lopez-Amo, M., Kolbeke, J., & Schuster, K. (2010). Interrogation of a Suspended-Core Fabry-Perot Temperature Sensor Through a Dual Wavelength Raman Fiber Laser. *Journal of Lightwave Technology* **28**(21), 3149-3155.

Rojas-Laguna, R., Hernández-García, J. C., Estudillo-Ayala, J. M., Ibarra-Escamilla, B., Pottiez, O., Vargas-Rodríguez, E., & Barrientos-García, A. (2015). Analysis of a low-cost technique for the generation of broadband spectra with adjustable spectral width in optical fibers. *Proc. SPIE*. **9347**, pp. 9347-9347-5.

Yang, X., Lu, Y., Liu, B., & Yao, J. (2017). Fiber Ring Laser Temperature Sensor Based on Liquid-Filled Photonic Crystal Fiber. *IEEE Sensors Journal* **17**(21), 6948-6952.

## Instructions for authors

A. Submission of papers to the areas of analysis and modeling problems of the current international society.

B. The edition of the paper should meet the following characteristics:

-Written in English. It is mandatory to submit the title and abstract as well as keywords. Indicating the institution of affiliation of each author, email and full postal address and identify the researcher and the first author is responsible for communication to the editor

-Print text in Times New Roman #12 (shares-Bold) and italic (subtitles-Bold) # 12 (text) and #9 (in quotes foot notes), justified in Word format. With margins 2 cm by 2 cm left-right and 2 cm by 2 cm Top-Bottom. With 2-column format.

-Use Calibre Math typography (in equations), with subsequent numbering and alignment right: Example;

$$\sigma \in \Sigma: H\sigma = \bigcap_{s < \sigma} Hs \quad (1)$$

-Start with an introduction that explains the issue and end with a concluding section.

- Items are reviewed by members of the Editorial Committee and two anonymous. The ruling is final in all cases. After notification of the acceptance or rejection of a job, final acceptance will be subject to compliance with changes in style, form and content that the publisher has informed the authors. The authors are responsible for the content of the work and the correct use of the references cited in them. The journal reserves the right to make editorial changes required to adapt the text to our editorial policy.

C. Items can be prepared by self or sponsored by educational institutions and business. The manuscript assessment process will comprise no more than twenty days from the date of receipt.

D. The identification of authorship should appear in a first page only removable in order to ensure that the selection process is anonymous.

E. Charts, graphs and figures support must meet the following:

-Should be self-explanatory (without resorting to text for understanding), not including abbreviations, clearly indicating the title and reference source with reference down with left alignment number 9 with bold typography.

-All materials will support gray scale and maximum size of 8 cm wide by 23 cm tall or less size, and contain all content editable.

- Tables should be simple and present relevant information. Prototype;



**Graph 1.** Three “Real” Indexes: Percent change from Their 2000 Peaks

F. References are included at the end of the document, all its components will be separated by a comma and must the following order:

- Articles: Kejun, Z. (2012). Feedback Control Methods for a New Hyperchaotic System. Journal of Information & Computational Science, No.9. Pp :231-237.

- Books: Barnsley, M. (1993). Fractals Everywhere. Academic Press. San Diego.

- WEB Resources: <http://www.worldfederationofexchanges.com>, see: (August, 16-2012)

The list of references should correspond to the citations in the document.

G. The notes to footnotes, which should be used and only to provide essential information.

H. Upon acceptance of the article in its final version, the magazine tests sent to the author for review. ECORFAN only accept the correction of typos and errors or omissions from the process of editing the journal fully reserving copyright and dissemination of content. Not acceptable deletions, substitutions or additions which alter the formation of the article. The author will have a maximum of 10 calendar days for the review. Otherwise, it is considered that the author (s) is (are) in accordance with the changes made.

I. Append formats Originality and Authorization, identifying the article, author (s) and the signature, so it is understood that this article is not running for simultaneous publication in other journals or publishing organs.

Taiwan \_\_\_\_ , \_\_\_\_ 20\_\_\_\_



**Originality Format**

I understand and agree that the results are final dictamination so authors must sign before starting the peer review process to claim originality of the next work.

---

Article

---

Signature

---

Name



Taiwan \_\_\_\_ , \_\_\_\_ 20 \_\_\_\_



**Authorization form**

I understand and accept that the results of evaluation are inappealable. If my article is accepted for publication, I authorize ECORFAN to reproduce it in electronic data bases, reprints, anthologies or any other media in order to reach a wider audience.

---

Article

---

Signature

---

Name

# ECORFAN Journal-Republic of Taiwán

## **Experimental investigation of a frequency swept laser based on erbium-doped fiber for applications in optical coherence tomography**

ARELLANO-ROMERO Silvia, BELTRAN-PEREZ, Georgina, CASTILLO, Mixcoatl, MUÑOZ-AGUIRRE, Severino, AVAZPOUR, Mahrokh, HERNANDEZ-GUTIERREZ, Ivan, RAMOS-BELTRAN, Jose de Jesus and MENDEZ-MARTINEZ, Hugo

*Benemérita Universidad Autónoma de Puebla*

## **Characterization of polarization-imbanced nonlinear loop mirror with input soliton pulses**

AVAZPOUR, Mahrokh, BELTRÁN-PÉREZ, Georgina, RODRÍGUEZ-MORALES Luis, ESCAMILLA IBARRA, Baldemar and KUZIN, Evgeny

*Benemérita Universidad Autónoma de Puebla*

*Instituto Nacional de Astrofísica, Óptica y Electrónica, Enrique Erro 1*

## **Supercontinuum generation study through the RK4IP method**

CARRILLO-DELGADO, Carlos Moisés, HERNANDEZ-GARCIA, Juan Carlos, ESTUDILLO-AYALA, Julian Moisés, LAUTERIO-CRUZ, Jesús Pablo, POTTIEZ, Olivier, MARTINEZ-ANGULO, José Ramón and ROJAS-LAGUNA, Roberto

*Universidad de Guanajuato*

*Cátedras CONACyT,*

*Centro de Investigaciones en Óptica*

## **A linear fiber laser temperature sensor based on a fiber Bragg grating**

REYES-AYONA, Jose Roberto, TORRES-GONZÁLEZ, Daniel, JÁUREGUI-VÁZQUEZ, Natalia, ESTUDILLO-AYALA, Julián Moisés, SIERRA-HERNÁNDEZ, Juan Manuel, JÁUREQUI-VÁZQUEZ, Daniel, HERNÁNDEZ-GARCÍA, Juan Carlos and ROJAS-LAGUNA, Roberto

*Universidad de Guanajuato*

